Nanoscale Advances

PAPER

View Article Online
View Journal | View Issue



Cite this: *Nanoscale Adv.*, 2025, **7**, 3406

# Molecular insight of nanosized Ba-Hao herbal ointment in accelerating chronic wound healing†

Han-Ying Qian,‡[a] Lu Chen,‡[bc] Xiao-Man Zhang,‡[a] Le Qiu,[b] Fei Wang,[b] Ting Feng,[d] Jie Shan, *[b] Xun Yuan *[d] and Xu-Lin Chen*[b]

Chronic wound treatment poses a substantial challenge to healthcare systems. Certain herbal medicines have demonstrated clinical efficacy in promoting chronic wound healing, yet their therapeutic mechanisms at the molecular level remain elusive due to their complex composition and multifaceted nature. In this study, Ba-Hao ointment (BHO), a sophisticated herbal formulation with diverse ingredients, is selected as a model to precisely investigate its wound-healing mechanism. Network pharmacology analysis and molecular docking simulations reveal that BHO specifically interacts with key wound-healing proteins, including vascular endothelial growth factor A (VEGFA), tumor necrosis factor-α (TNF-α), and interleukin-1β (IL-1β), suggesting its ability to modulate critical biological pathways involved in inflammation and tissue regeneration. Experimental validation further demonstrates that BHO significantly promotes cell proliferation, suppresses bacterial infection, and enhances the expression of essential growth factors such as epidermal growth factor (EGF) and VEGFA in normal human dermal fibroblasts (NHDF), all of which are vital for effective wound healing. *In vivo* studies confirm that BHO accelerates wound closure, reduces inflammation, and promotes the development of well-organized granulation tissue *via* activation of the PI3K-Akt signaling pathway. This study is interesting since it unveils BHO's molecular role in chronic wound healing, furthering herbal medicine development and insights.

Received 28th December 2024
Accepted 11th April 2025

DOI: 10.1039/d4na01075b

rsc.li/nanoscale-advances



## 1. Introduction

Chronic wounds, which fail to restore anatomical and functional integrity through the normal, orderly repair process, present a significant challenge to healthcare systems due to their high incidence, prevalence, and associated costs.[1–4] Affecting the quality of life of approximately 2.5% of the global population, these wounds impose a considerable economic burden. With an aging population, rising prevalence of diabetes and obesity, and persistent infection risks,[5,6] chronic wounds are expected to remain a profound clinical, social, and economic concern.[7–9] Chronic wounds are characterized by persistent inflammation, elevated levels of pro-inflammatory cytokines, reactive oxygen species (ROS),[7] and senescent cells, all of which obstruct the healing process.[10,11] Currently, primary treatment methods in clinical settings typically involve antibiotics, Ag ion dressings,[12,13] and herbal medicines.[14,15] While antibiotics and Ag ion dressings are effective in inhibiting bacterial infections,[4,16–18] issues such as antibiotic resistance and limited acceptance of heavy metals for Ag ion dressings, as well as their ineffectiveness in anti-inflammation[19] and ROS elimination,[20] may limit their practical applications. In contrast, herbal medicines have been widely used for chronic wound treatment for thousands of years and demonstrated to effectively promote healing without concerns of drug resistance or heavy metal ion poisoning.[21–23] As a result, they have become a commonly used strategy for chronic wound treatment in many countries, such as China.[24–26] However, several issues arise during the clinical application of herbal medicines.[27–30] Particularly, due to their multi-component nature and complex interactions with wound sites, the molecular-level mechanisms of herbal medicines for chronic wound healing remain unclear.[31–33] The bulk and multi-component nature of herbal remedies make it difficult to conduct scientific research on these mechanisms.[34–36] Resolving these problems can provide insights for future herbal formulation optimization and act as a model for the creation and mechanistic study of herbal medications.

[a]*Anhui University of Chinese Medicine, Hefei, Anhui 230038, China*
[b]*Department of Burns, The First Affiliated Hospital of Anhui Medical University, Hefei, Anhui 230022, China. E-mail: okcxl@126.com; shanjie@ahmu.edu.cn*
[c]*Department of Integrated Traditional Chinese and Western Medicine, Anhui Medical University, Hefei, Anhui 230032, China*
[d]*School of Material Science and Engineering, Qingdao University of Science and Technology, Qingdao, Shandong 266042, China. E-mail: yuanxun@qust.edu.cn*

† Electronic supplementary information (ESI) available. See DOI: https://doi.org/10.1039/d4na01075b

‡ Han-Ying Qian, Lu Chen, and Xiao-Man Zhang contributed equally to this work and are joint first authors.

Among the many herbal remedies, BaHao Ointment (BHO), created by Anhui Medical University's First Affiliated Hospital, has been widely used for wound care, including the treatment of chronic wounds, and has been shown to be effective in accelerating healing in tens of thousands of instances. For this reason, BHO is a great herbal model for studying chronic wound healing at the molecular level. Rhubarb, *Sanguisorba officinalis*, gallnut, and borneol are the main components of BHO and contain significant amounts of plant material.[37,38] These large-sized components may hinder the active compounds' ability to permeate cells effectively. Nanomaterials have been proved to be capable of preventing the formation of biofilms by microorganisms, so it has better anti-infection effect. Meanwhile, nanomaterials can facilitate wound healing by promoting wound repair cell proliferation and angiogenesis.[39–42] Nanotechnology could address this issue by milling these large-sized components into nanosized particles, potentially enhancing their penetration through the skin to the lesion site, thereby ensuring both healing efficacy and therapeutic precision. Nevertheless, it is still unknown if BHO has antibacterial, anti-inflammatory, and cell proliferative actions all at once. Therefore, elucidating the molecular-level mechanisms underlying BHO's effectiveness is the primary motivation for this study.[43,44]

Herein we report the findings on the molecular mechanisms underlying the efficacy of BHO in treating chronic wounds. As shown in Fig. 1, network pharmacology analysis initially reveals BHO's interactions with key wound healing proteins such as vascular endothelial growth factor A (VEGFA), tumor necrosis factor-α (TNF-α) and interleukin-1β (IL-1β). These interactions highlight BHO's potential to influence key biological pathways associated with inflammation and tissue regeneration, shedding light on its possible mechanism of action in chronic wound treatment. According to experimental confirmation, BHO dramatically increases cell proliferation, suppresses bacterial infection, and causes normal human dermal fibroblasts (NHDF) to upregulate critical growth factors like VEGFA and epidermal growth factor (EGF), all of which are necessary for efficient wound healing. *In vivo* results from a chronic wound mouse model show that BHO markedly accelerates wound closure, reduces inflammation, and promotes organized granulation tissue formation *via* the PI3K-Akt signaling pathway. This study is noteworthy as it not only uncovers the molecular mechanisms of BHO in chronic wound treatment but also advances the development and mechanistic understanding of herbal medicines.

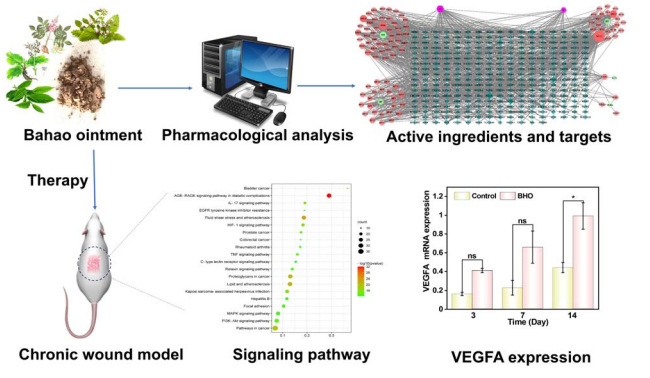


Fig. 1 Schematic illustration of the mechanistic analysis of BHO for chronic wound treatment.

## 2. Experimental

### 2.1 Preparation of nano-sized BHO

The Chinese herbal medicine powder, BHO, was processed using a high-energy ball mill (Retsch, Germany). The material was milled at room temperature with a rotational speed of 600 rpm for a duration of 20 minutes, resulting in particle sizes of less than 100 nm.

### 2.2 Identification of active ingredients and targets of BHO

The bioactive components of BHO and their target interactions were extracted from the Traditional Chinese Medicines Integrated Database (TCMID, **https://47.100.169.139/tcmid/**) and the Traditional Chinese Medicine Systematic Pharmacology Database (TCMSP, **http://www.tcmspw.com/tcmsp.php**). The UniProt database (**https://www.uniprot.org/**) was utilized to standardize target names, specify the species as "human," and convert all retrieved proteins to UniProt IDs to identify potential targets of BHO compounds.

### 2.3 Identification of predicted targets of BHO during wound healing

The GeneCards database (**https://www.genecards.org/**) was accessed to identify disease targets associated with "wound healing," specifically focusing on entries with a relevance score greater than 3.0.

### 2.4 Molecular docking (MD)

The 3D molecular structures of the core components were obtained from the TCMSP database, while the target proteins corresponding to the core genes in the protein–protein interaction (PPI) network were retrieved from the PDB database (**https://www.rcsb.org/**). The protein structure was then prepared using AutoDock Tool 1.5.6 software, where water molecules were removed, and hydrogen atoms were added. The protein was designated as the receptor, and the structure was saved in the PDBQT format. This format was used to compute the minimal binding energy, and OpenBabelGUI software was employed to convert the composite from PDBQT to PDB format. Finally, docking results were visualized using the PyMol 2.4 molecular visualization system.

### 2.5 Animal experiments

A full-thickness skin defect model was established in C57BL/6J mice to evaluate the therapeutic effect of BHO on chronic refractory wounds. Eighteen mice were housed with free access to food and water and randomly divided into a control group and a BHO group. All mice were anesthetized with 1.25% tribromoethanol, and chronic wounds were induced on their dorsal skin by creating full-thickness defects followed by

intramuscular injection of hydrocortisone sodium succinate (8 mg/100 g). Post-modeling, mice were individually caged. The control group received PBS treatment, while the BHO group was treated with BHO. Dressings were changed every two days. Wound size was photographed and measured at days 0, 3, 7, and 14, and the healing rate was calculated. Histological analysis of wound tissue was performed using hematoxylin and eosin (H&E) staining and Masson staining. Additionally, mRNA and protein expression levels of matrix metalloproteinase-8 (MMP8) and VEGFA in the wounds were quantified. Animal experiments were approved by the Ethics Committees of Anhui Medical University and Anhui University of Chinese Medicine and were performed in strict accordance with the NIH guidelines for the care and use of laboratory animals (NIH Publication No. 85-23 Rev. 1985). All surgeries were performed under anesthesia, and efforts were made to minimize suffering.

# 3. Results and discussion

## 3.1 Material characterization

Before conducting a mechanistic investigation of BHO for chronic wound treatment, the large-sized ingredients of BHO were reduced to nanosized particles through ball milling. The processed BHO is seen as a solid, brownish-yellow powder in the inset of Fig. 2a. Scanning electron microscopy (SEM) analysis was employed to examine the morphology of BHO (Fig. 2a), revealing an average particle size of approximately 100 nm, which facilitates the release of active components into the surrounding environment. Further SEM mapping analysis in Fig. 2b–g showed that BHO contains a uniform distribution of non-metallic elements such as carbon, nitrogen, oxygen, phosphorus, and sulfur. These ingredients are part of the herbal formula's active ingredients and are crucial for its antioxidant and anti-inflammatory properties. The absence of metallic components indicates that BHO does not pose a risk of heavy metal toxicity. Additionally, Fourier-transform infrared (FTIR) spectrum (Fig. 2h) revealed five distinct characteristic absorption peaks (3442.39 $cm^{-1}$, 2925.71 $cm^{-1}$, 1630.76 $cm^{-1}$, 1349.05 $cm^{-1}$, and 1032.14 $cm^{-1}$), which correspond to the stretching vibration of hydroxyl groups (–OH), C–H stretching vibration, C=C double bond stretching vibration or aromatic ring vibration modes, C–H deformation vibration or C–O stretching vibration, and C–H deformation vibration or C–O stretching vibration and C–C stretching vibration. These results suggest that BHO contains a variety of active components, such as ester compounds, flavonoids, tannins, and gallic acid and so on. Contact angle tests in Fig. 2i revealed a water contact angle of 129.1°, indicating that BHO is hydrophobic, which can prevent the hydrolysis and oxidation of active components. These characterization analyses demonstrate that BHO has particle sizes around 100 nm, contains some non-metallic elements (*i.e.*, C, N, O, P, and S) with specific chemical bonds, and exhibits hydrophobic properties, providing a solid foundation for its subsequent applications.

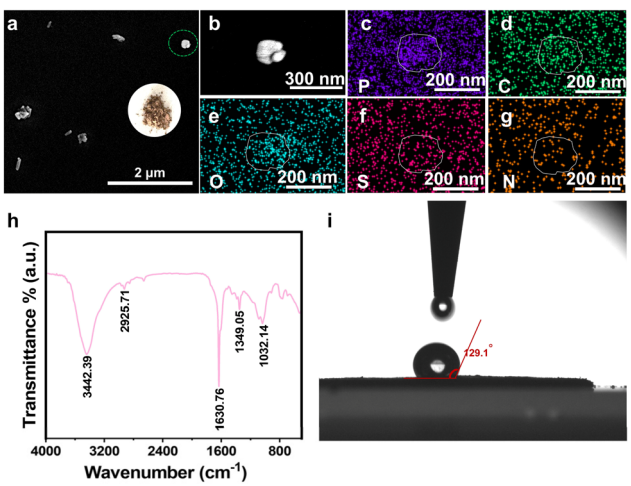


Fig. 2 (a) SEM image of BHO, inset: the photograph of BHO powders. The nanoscale particle size of BHO powders can facilitate the release of their active components. (b–g) SEM elemental mapping of BHO: (c) phosphorus element, (d) carbon element, (e) oxygen element, (f) sulfur element, (g) nitrogen element. These non-metallic elements contribute to the active components of the herbal formula, playing an important role in anti-inflammatory and antioxidant activities. (h) FTIR spectrum of BHO, suggesting that BHO contains a variety of active components. (i) Photograph of the water contact angle. It indicates that hydrophobic BHO can prevent the hydrolysis and oxidation of active components.

## 3.2 Pharmacological analysis and molecular docking analysis of BHO

The BHO is a sophisticated formulation, intricately composed of diverse herbs, serving as both a nanomaterial and a traditional Chinese medicine (TCM) compound. The complex pharmacological profile of TCM, marked by diverse bioactive components and multifaceted targets, creates extensive therapeutic pathways, posing significant challenges for comprehensive research. To address this, we employed network pharmacology analysis to investigate BHO, aiming to provide a robust scientific foundation and a systematic elucidation of the mechanisms underpinning BHO therapies. Typically, the bioactive compounds of BHO including *Rheum palmatum* (Dahuang), *Sanguisorba officinalis* (Diyi), borneol (Bingpian), *Lapis lithanthrax* (Luganshi), *Galla chinensis* (Wubeizi), and haematite (Chishizhi), along with their corresponding target proteins, were extracted from various databases (Fig. 3a). Notably, Chishizhi is categorized in TCM as an herb similar to Wubeizi, both of which are known for their wound-healing capabilities, suggesting that their molecular targets may overlap even if no particular targets were found in the TCMID or TCMSP databases. The network pharmacology analysis results demonstrated that the formulation's multi-component, multi-target characteristics were depicted in the component-target network, comprising 402 nodes (with 302 nodes functioning as drug targets) and 1100 edges. In the network diagram (Fig. 3a), the dark green rectangular region represents potential therapeutic targets of BHO, while the light green circles represent the individual herbs (Dahuang, Diyi, Bingpian, Luganshi, and Wubeizi). Surrounding each herb are pink edges, which

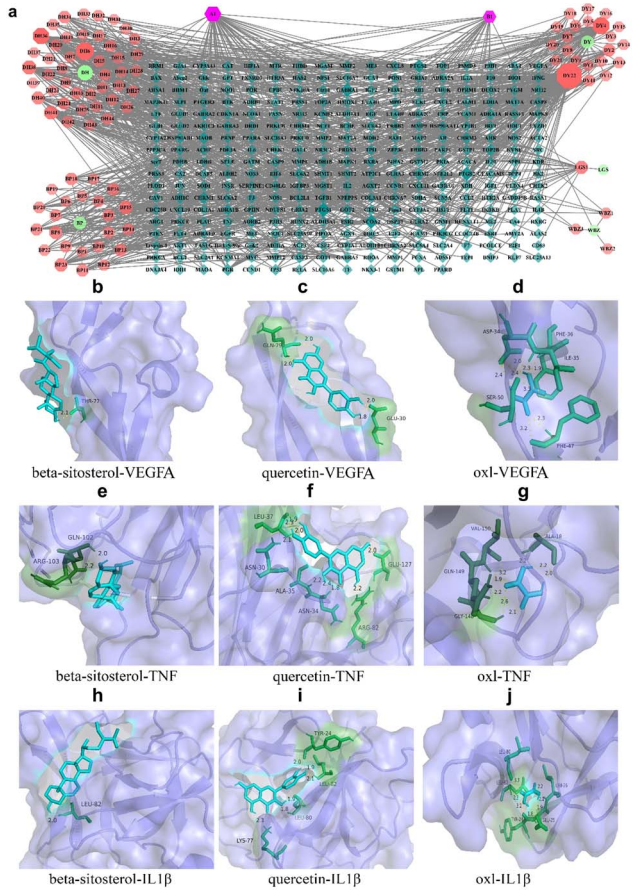


Fig. 3 (a) The composite target network diagram of BHO. Note: the formulation has multi-component, multi-target characteristics in the component-target network, comprising 402 nodes (labelled with dark green color in the central area; with 302 nodes functioning as drug targets) and 1100 edges; the five light green dots at the periphery represent Chinese herbs, namely, Dahuang (DH), Bingpian (BP), Luganshi (LGS), Diyi (DY) and Wubeizi (WBZ), with their corresponding components in light pink at their periphery and A1 and B1 in purple for their shared components. Molecular docking diagram of active components and key targets in BHO. (b) β-Sitosterol-VEGFA, (c) quercetin-VEGFA, (d) oxl-VEGFA, (e) quercetin-TNF, (f) oxl-TNF, (g) β-sitosterol-TNF, (h) quercetin-IL-1β, (i) oxl-IL-1β, and (j) β-sitosterol-IL-1β. These bioactive components constitute the mechanistic foundation for BHO's wound-healing efficacy by regulating inflammatory signalling pathways.

correspond to the active ingredients associated with those herbs. The purple A1 and B1 markers indicate overlapping active ingredients between the herbs. The size and color of the nodes represent the degree of interaction, with larger and darker nodes indicating higher degree values. The top three active ingredients, based on degree value, were identified as quercetin, *Oxalis corniculata* L. (oxl, a main ingredient from oxalis), and β-sitosterol (Table S1†).

Subsequently, we utilized AutoDock software to conduct molecular docking simulations for the top three active compounds—quercetin, oxl, and β-sitosterol—against the core genes identified as key targets in the formulation: VEGFA, TNF-α, and IL-1β. The molecular docking simulations allowed for the calculation of the minimum binding energy for each active compound–target interaction. The docking visualizations presented in Fig. 3b–j illustrate the interactions between the active compounds and their corresponding targets: β-sitosterol-VEGFA, quercetin-VEGFA, oxl-VEGFA, quercetin-TNF-α, oxl-TNF-α, β-sitosterol-TNF-α, quercetin-IL-1β, oxl-IL-1β, and β-sitosterol-IL-1β. The molecular docking results (Table S2†) indicate that the binding energies for all interactions were less than 0 kJ $mol^{-1}$, suggesting that the components of BHO exhibit favorable binding affinities with these wound-healing targets. A greater absolute value of binding energy indicates a stronger affinity and improved docking efficiency, highlighting the potential therapeutic efficacy of BHO in promoting wound healing and modulating inflammation.

### 3.3 Cell proliferation and expression of EGF and VEGFA *in vitro*

To assess the impact of BHO on the proliferation of NHDF, we conducted cell co-incubation and measured changes in optical density at 450 nm ($OD_{450}$). Additionally, we quantified these factors using quantitative Real-Time Polymerase Chain Reaction (qRT-PCR) (Fig. 4). In the Fig. 4a, compared to the control group, BHO concentrations of 100 μg $mL^{-1}$ and 300 μg $mL^{-1}$ significantly promoted the proliferation of NHDF ($p < 0.01$). However, at a concentration of 1000 μg $mL^{-1}$, BHO inhibited cell proliferation. Based on these findings, it has been determined that the safe dosage of BHO for therapeutic use is below 1000 μg $mL^{-1}$. Given that EGF and VEGFA are two critical therapeutic indicators essential for promoting chronic wound healing, we investigated the effects of various concentrations of BHO on the expression of these two factors in NHDF, with the results presented in Fig. 4b and c qRT-PCR analysis revealed that, compared to the control group, treatment with BHO at a concentration of 100 μg $mL^{-1}$ significantly increased the expression of EGF and VEGFA in normal human skin fibroblasts ($n = 3$, $p < 0.01$). However, at drug concentrations below 100 μg $mL^{-1}$, there were no significant changes in the expression levels of VEGFA and EGF.

### 3.4 Amelioration of chronic wound by BHO treatment

During the treatment of chronic wounds, bacterial infection is a significant obstacle to wound healing, prompting us to explore the antibacterial properties of BHO. As illustrated in

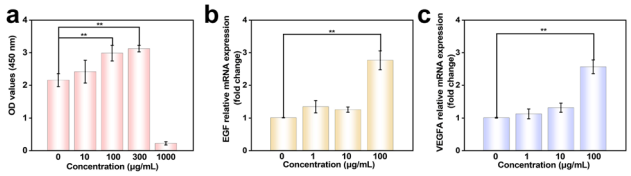


Fig. 4 (a) Optical density (OD) values of NHDF cells stimulated by different BHO concentrations for 48 hours. The mRNA expressions of (b) EGF and (c) VEGFA in different BHO concentrations groups. Results are expressed as mean ± standard deviation ($n = 3$), $^{**}p < 0.01$ *vs.* control, one-way ANOVA.

Fig. S1,† as the concentration of BHO increased, the number of bacteria on the agar plates progressively decreased, demonstrating BHO's antibacterial efficacy in promoting wound recovery. To delve into the molecular-level mechanism of BHO in chronic wound healing, we also evaluated the therapeutic effects of BHO using a mouse model of chronic wounds (Fig. 5). As depicted in Fig. 5a, after three days of treatment, the control group mice exhibited noticeable secretions on the wound surface, substantial tissue edema, and a fresh color at the wound base, but no granulation tissue had formed. Conversely, the BHO group displayed minimal secretion, no significant edema, a fresh base color, and the initiation of granulation tissue formation. By day 7, the wound area in the control group had decreased compared to day 3. A small amount of secretion and persistent edema were still present, along with only a limited formation of granulation tissue. In contrast, the wound area in the BHO group exhibited a reduction in size, characterized by minimal secretion, no edema, and a scab covering the surface. Upon removal of the scab, a greater amount of granulation tissue was observed. By day 14, the control group's wound displayed only minimal new hair growth and scab attachment. In contrast, the wound area in the BHO group was covered with new hair and was nearly healed. These findings indicate that the BHO group experienced less edema and secretion during the healing process, as well as accelerated granulation tissue formation and wound healing, demonstrating significant improvements compared to the control group. The wound healing rates of the two groups of mice on day 3 were significantly lower than those on days 7 and 14, with statistically significant differences ($p < 0.05$) (Fig. 5b). The healing rates in the BHO group on day 7 and day 14 were higher than those in the control group, and the differences were statistically significant ($p < 0.01$).

After the treatment, the skin at the wound site was examined histologically, as illustrated in Fig. 5c and d. On day 3 post-modeling, the wounds exhibited significant infiltration of inflammatory cells, predominantly lymphocytes. There was no evidence of capillary formation, and the fibroblasts appeared disorganized. By day 7 post-modeling, the BHO group demonstrated a reduction in inflammatory cells, the presence of visible capillary formation, and a more organized alignment of fibroblasts compared to earlier observations. Conversely, the control group also showed a decrease in inflammatory cells; however, their numbers remained relatively high, with fewer and disorganized fibroblasts. By day 14 post-modeling, the BHO group demonstrated a significant reduction in inflammatory cells and neatly arranged capillaries; however, the control group had more inflammatory cells and disorganized fibroblast alignment compared to the BHO group.

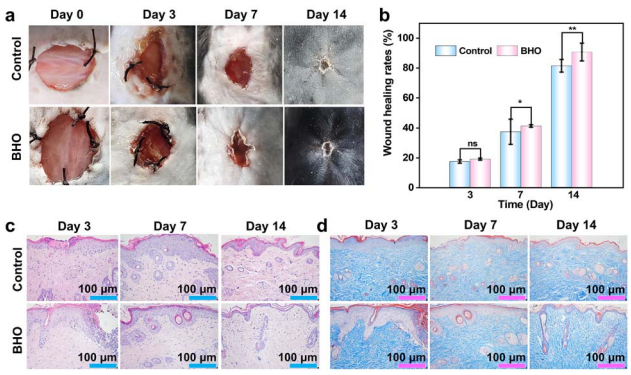


Fig. 5 (a) Photos of mouse chronic wounds treated with BHO or PBS as control at day 0, 3, 7, and 14. (b) Corresponding wound healing rates. (c) H&E staining, and (d) Masson's trichrome staining of the harvested skin from the control group and BHO group. Results are expressed as mean ± standard deviation ($n = 3$), *$p < 0.05$, **$p < 0.01$ *vs.* control, one-way ANOVA.

### 3.5 Mechanism analysis of BHO for the chronic wound at the gene level

Subsequently, the skin samples from the control group and the BHO group of mice were sent for RNA transcriptome testing, with the analysis information listed in Fig. 6. The Venn diagram (Fig. 6a) shows that there are 203 and 517 wound-related genes in the control and BHO groups, respectively, with 99 genes common to both groups. This finding indicates that BHO can regulate the expression of wound-related genes. Further analysis of gene ontology (GO) is shown in Fig. 6b. In the GO analysis, 10 biological functions, cellular functions, and molecular functions were selected. The *x*-axis represents the function of the genes and the *y*-axis indicates the number of target genes. As shown in Fig. 6b, these functions are associated with biological processes, including the positive regulation of transcription from the RNA polymerase II promoter, negative regulation of apoptosis, cellular response to lipopolysaccharide, and positive regulation of angiogenesis.

To explore the signaling pathway mechanisms of BHO in wound healing, a Kyoto Encyclopedia of Genes and Genomes (KEGG) enrichment analysis was conducted. As shown in Fig. 6c, the top 20 signaling pathways are displayed. The size of the bubbles represents the number of target proteins, with larger bubbles indicating more proteins and smaller bubbles indicating fewer. The color of the bubbles represents the *p*-value; darker colors indicate smaller *p*-values, thus greater relevance. According to the number of enrichments and *p*-values, the pathways affected by the BHO ointment likely involve the HIF-1, IL-17, TNF, PI3K-Akt and other signaling pathways. These pathways are related to inflammatory pathology, cell metabolism, growth, and development, with most intersected genes enriched in these pathways. Among them, the PI3K-Akt pathway is an intracellular signal transduction pathway that responds to extracellular signals, promotes metabolism, proliferation, cell survival, growth, and angiogenesis, which is also a common pathway related to wound healing.

Therefore, the PI3K-Akt signaling pathway is further utilized to deeply investigate and explore the mechanisms of wound healing. The phosphorylated Akt1/2/3 (p-Akt1/2/3) and Akt1/2/3 (including p-Akt1/2/3 and non-p-Akt1/2/3) are important components of this signaling pathway, where an increase in p-Akt1/2/3 expression can more effectively activate fibroblasts.

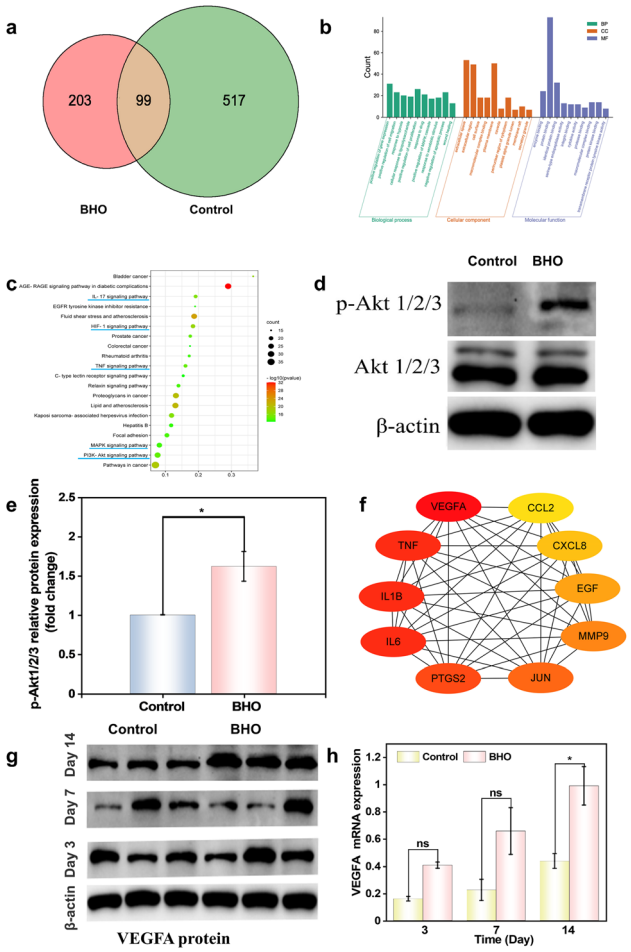


Fig. 6 (a) Venn diagram between the targets of BHO and the targets associated with wound healing, (b) gene ontology (GO) enrichment analysis for key targets (top 10 listed), (c) KEGG pathway enrichment analysis for key targets (top 20 listed), (d) western blots for phosphorylated Akt (p-Akt 1/2/3) and total Akt (Akt 1/2/3), (e) quantification of the western blot results from (d), (f) the protein–protein interaction (PPI) network of BHO and wound healing targets, on days 3, 7, and 14 in mouse skin, (g) western blot of VEGFA protein, and (h) VEGFA mRNA expression levels. Results are expressed as mean ± standard deviation ($n = 3$), *$p < 0.05$, *vs.* control, one-way ANOVA.

Western blot (WB) analysis was employed to assess the levels of Akt1/2/3 and p-Akt1/2/3 (Fig. 6d and e), revealing that BHO treatment significantly elevated the levels of p-Akt1/2/3 proteins ($p < 0.05$), while the total Akt1/2/3 protein levels remained unchanged. This suggests that BHO effectively modulates the PI3K-Akt signaling pathway by enhancing the activation of p-Akt1/2/3. Additionally, a protein–protein interaction (PPI) analysis was performed on the 99 common genes identified in Fig. 6a, highlighting key proteins such as VEGFA, TNF-α, IL-1β, and IL-6. In this analysis, nodes represent individual proteins, with the color of the nodes shifting from pink to red, indicating the degree of binding between proteins; the darker the color, the higher the interaction strength. Edges represent associations between proteins. The analysis identified VEGFA as a central protein in the network. Subsequently, the expression of VEGFA protein and mRNA were measured in the skin of mice from the control and BHO groups over different days, with the results displayed in Fig. 6g and h. By day 14, the expression levels of both VEGFA protein and mRNA were higher in the skin of mice from the BHO group, confirming that BHO accelerates the healing of chronic wounds by increasing the levels of VEGFA. To comprehensively assess the recovery stages during the wound healing process, this study characterized the expression of MMP-8 using qRT-PCR, with results displayed in Fig. S2.† The expression of MMP-8 in the skin of both mouse groups showed a trend of increasing initially and then decreasing. Notably, at the inflammation stage (day 7), the MMP-8 expression in the BHO group was significantly higher than that in the control group. This finding suggests that BHO can enhance MMP-8 expression, thereby accelerating the clearance of damaged tissue and foreign invaders, which facilitates early wound healing.

## 4. Conclusions

In summary, we have conducted molecular-level studies to reveal mechanisms underlying the efficacy of BHO in treating chronic wounds. BHO has been evaluated as an effective remedy for chronic wounds, characterized by its nanoscale, non-toxic properties, rich non-metallic composition, and unique surface chemistry. Based on network pharmacology analysis, specific interactions were identified between BHO and several key wound healing proteins, including VEGFA, TNF-α, and IL-1β. This suggests that BHO has the potential to influence critical biological pathways associated with inflammation and tissue regeneration in the treatment of chronic wounds. Experimental validation revealed that BHO substantially stimulates cell proliferation, inhibits bacterial infection, and upregulates key growth factors such as EGF and VEGFA in NHDF, all of which are crucial for optimal wound healing. *In vivo* studies further demonstrated that BHO significantly accelerates wound closure, mitigates inflammation, and fosters the formation of well-structured granulation tissue through the PI3K-Akt signaling pathway. This study is significant since it unveils BHO's molecular role in chronic wound healing, furthering herbal medicine development and insights.

## Data availability

The data that support the findings of this study are available on request from the corresponding author.

## Conflicts of interest

The authors declare no conflicts of interest in relationship to this study.

## Acknowledgements

This work was supported by the National Natural Science Foundation of China (Grant no. 82372517 and 82172204) and a construction foundation of Department of Integrated Traditional and Western Medicine of the First Affiliated Hospital of

Anhui Medical University (Grant no. 9001001853). The animal experiments followed the NIH guidelines for animal care and use (NIH Publication No. 85-23 Rev. 1985) and received approval from the Biomedical Ethics Committees of Anhui Medical University and Anhui University of Chinese Medicine (Hefei, China).

## References

1 Y. Z. Wei, T. Xu, C. Wang, S. Liu, W. Zhang, J. Sun, H. Yu, H. Shi and Y. Song, A hydrogel-functionalized silver nanocluster for bacterial-infected wound healing, *Nanoscale*, 2024, **16**, 10656.

2 B. Wu, W. Pan, S. Luo, X. Luo, Y. Zhao, Q. Xiu, M. Zhong, Z. Wang, T. Liao, N. Li, C. Liu, C. Nie, G. Yi, S. Lin, M. Zou, B. Li and L. Zheng, Turmeric-derived nanoparticles functionalized aerogel regulates multicellular networks to promote diabetic wound healing, *Adv. Sci.*, 2024, **11**, e2307630.

3 Y. Hu, H. Li, X. Lv, Y. Xu, Y. Xie, L. Yuwen, Y. Song, S. Li, J. Shao and D. Yang, Stimuli-responsive therapeutic systems for the treatment of diabetic infected wounds, *Nanoscale*, 2022, **14**, 12967.

4 R. Song, H. Xie and G. Liu, Advances of MXene-based hydrogels for chronic wound healing, *Chin. Chem. Lett.*, 2025, DOI: **10.1016/j.cclet.2024.110442**.

5 Z. Fang, S. Zhang, W. Wang, Y. Xu, M. Lu, Y. Qian, X. Xiao, Y. Li, B. Z. Tang and M. Zhang, Aggregation-induced emission-based phototheranostics to combat bacterial infection at wound sites: A review, *Biomaterials*, 2025, **315**, 122950.

6 Y. Qiao, Y. Ping, H. Zhang, B. Zhou, F. Liu, Y. Yu, T. Xie, W. Li, D. Zhong, Y. Zhang, K. Yao, H. A. Santos and M. Zhou, Laser-activatable CuS nanodots to treat multidrug-resistant bacteria and release copper ion to accelerate healing of infected chronic nonhealing wounds, *ACS Appl. Mater. Interfaces*, 2019, **11**, 3809.

7 M. Kumi, T. Chen, Z. Zhang, A. Wang, G. Li, Z. Hou, T. Cheng, J. Wang, T. Wang and P. Li, Integration of hydrogels and 3D bioprinting technologies for chronic wound healing management, *ACS Biomater. Sci. Eng.*, 2024, **10**, 5995.

8 J. Deng, G. Shi, Z. Ye, Q. Xiao, X. Zhang, L. Ren, F. Yang and M. Wang, Unveiling and swift diagnosing chronic wound healing with artificial intelligence assistance, *Chin. Chem. Lett.*, 2025, DOI: **10.1016/j.cclet.2024.110496**.

9 T. Li, H. Zhu and Z. Wu, Viewing aggregation-induced emission of metal nanoclusters from design dtrategies to applications, *Nanomaterials*, 2023, **13**, 470.

10 S. Ai, Y. Li, H. Zheng, M. Zhang, J. Tao, W. Liu, L. Peng, Z. Wang and Y. Wang, Collision of herbal medicine and nanotechnology: a bibliometric analysis of herbal nanoparticles from 2004 to 2023, *J. Nanobiotechnol.*, 2024, **22**, 140.

11 S. Feng, X. Peng, Y. Deng, Y. Luo, S. Shi, X. Wei, X. Pu and X. Yu, Biomimetic nanozyme-decorated smart hydrogel for promoting chronic refractory wound healing, *ACS Appl. Mater. Interfaces*, 2024, **16**, 59862.

12 N. Ninan, N. Goswami and K. Vasilev, The impact of engineered silver nanomaterials on the immune system, *Nanomaterials*, 2020, **10**, 967.

13 K. Zheng and J. Xie, Cluster materials as traceable antibacterial agents, *Acc. Mater. Res.*, 2021, **2**, 1104–1116.

14 S. Zhou, X. Hu, Y. Wang, W. Fei, Y. Sheng and H. Que, The global prevalence of methicillin-resistant staphylococcus aureus in patients with diabetic foot ulcers: A systematic review and meta-analysis, *Diabetes, Metab. Syndr. Obes.: Targets Ther.*, 2024, **17**, 563–574.

15 F. Jiao, W. Zhao, W. Zhao, Y. Wang, Y. Deng, S. Chang, J. Sun, Q. Lou, L. Wang, C. X. Shan, Y. Xiao and L. Dong, Biomass-derived washable composites for accelerating the healing of infected wounds, *BMEMat*, 2023, **1**, e12055.

16 J. Xu, L. Chang, Y. Xiong and Q. Peng, Chitosan-based hydrogels as antibacterial/antioxidant/anti-Inflammation multifunctional dressings for chronic wound healing, *Adv. Healthcare Mater.*, 2024, 202401490.

17 S. Sucharita Singh, B. Jena, S. Roy, S. Nayak, S. K. Behera, S. Chakrabortty, S. K. Tripathy, M. Ali Khan, R. Kumar, B. H. Jeon, C. Stålsby Lundborg and A. Mishra, Sprayable biogenic Ag-collagen nanocomposites with potent antibacterial and antibiofilm activity for *Acinetobacter baumannii* infected wound healing under hyperglycemic condition, *Chem. Eng. J.*, 2024, **490**, 151788.

18 L. Han, Z. Yuan, H. M. Ren, W. Song, R. Wu, J. Li, Z. Guo, B. Yu, S. Duan and F. J. Xu, Infection-responsive polysaccharide-based drug-loaded nano-assembly for dual-modal treatment against drug-resistant bacterial lung infection, *BMEMat*, 2024, **2**, e12082.

19 W. Wang, Y. Gao, Y. Lin, Y. Qian, J. Shen, N. Zhou, B. Z. Tang and M. Zhang, Inflammatory microenvironment-responsive nanomotors with NIR photothermal effect for deep inflammation elimination and infection inhibition, *Adv. Funct. Mater.*, 2024, 202416684.

20 C. Geng, S. He, S. Yu, H. M. Johnson, H. Shi, Y. Chen, Y. K. Chan, W. He, M. Qin, X. Li and Y. Deng, Achieving clearance of drug-resistant bacterial infection and rapid cutaneous wound regeneration using an ROS-balancing-engineered heterojunction, *Adv. Mater.*, 2024, **36**, 2310599.

21 Y. Guo, C. Yuan, T. Huang and Z. Cheng, Integrating UHPLC-Q-TOF-MS/MS, network pharmacology, bioinformatics and experimental validation to uncover the anti-cancer mechanisms of TiaoPi AnChang decoction in colorectal cancer, *J. Ethnopharmacol.*, 2024, **334**, 118576.

22 Y. Song, N. Han, Z. Guo, H. Li, M. Guo, M. Dou, J. Ye, Z. Peng, X. Lu, M. Li, X. Wang, J. Bai and S. Du, Baicalein-modified chitosan nanofiber membranes with antioxidant and antibacterial activities for chronic wound healing, *Int. J. Biol. Macromol.*, 2024, **279**, 134599.

23 Y. Wang, Y. Sui, J. Yao, H. Jiang, Q. Tian, Y. Tang, Y. Ou, J. Tang and N. Tan, Herb-CMap: a multimodal fusion framework for deciphering the mechanisms of action in

traditional Chinese medicine using Suhuang antitussive capsule as a case study, *Briefings Bioinf.*, 2024, **25**, bbae362.
24 W. Wu, B. Zhang, W. Wang, Q. Bu, Y. Li, P. Zhang and L. Zeng, Plant-derived exosome-like nanovesicles in chronic wound healing, *Int. J. Nanomed.*, 2024, **19**, 11293.
25 Y. Xue, W. Zhu, F. Qiao, Y. Yang, J. Qiu, C. Zou, Y. Gao, X. Zhang, M. Li, Z. Shang, Y. Gao and L. Huang, Ba-Qi-Rougan formula alleviates hepatic fibrosis by suppressing hepatic stellate cell activation via the MSMP/CCR2/PI3K pathway, *J. Ethnopharmacol.*, 2024, **329**, 118169.
26 Z. Zhen, S. Wei, F. W. Yun, X. Jie, N. X. Jie, T. S. Yi, X. Wen, Y. G. Shu, L. Yue, Y. W. Xuan, M. Z. Yu and F. Q. Hua, Astragalus polysaccharide improves diabetic ulcers by promoting M2-polarization of macrophages to reduce excessive inflammation via the β-catenin/NF-κB axis at the late phase of wound-healing, *Heliyon*, 2024, **10**, e24644.
27 I. P. Maksum, R. Rustaman, Y. Deawati, Y. Rukayadi, A. R. Utami and Z. K. Nafisa, Study of the antidiabetic mechanism of berberine compound on FOXO1 transcription factor through molecular docking and molecular dynamics simulations, *J. Mol. Modell.*, 2024, **30**, 260.
28 B. Ravindhran, N. Schafer, A. Howitt, D. Carradice, G. Smith and I. Chetter, Molecular mechanisms of action of negative pressure wound therapy: a systematic review, *Expert Rev. Mol. Med.*, 2023, **25**, e29.
29 S. Y. Xu, H. Y. Cao, R. H. Yang, R. X. Xu, X. Y. Zhu, W. Ma, X. B. Liu, X. Y. Yan and P. Fu, Genus Paeonia monoterpene glycosides: A systematic review on their pharmacological activities and molecular mechanisms, *Phytomedicine*, 2024, **127**, 155483.
30 D. Yang, Z. Li, Y. Peng, X. Zhu, J. Gong and C. Chen, Network pharmacology combined with molecular docking simulations reveal the mechanism of action of Glycyrrhiza for treating pneumonia, *Pept. Sci.*, 2024, **116**, e24342.
31 L. Luo, J. Zhou, X. Liu, Y. Chen, X. Du, L. Gao, Y. Sun and S. Wang, Development of modern Chinese medicine guided by molecular compatibility theory, *J. Adv. Res.*, 2025, DOI: **10.1016/j.jare.2024.08.005**.
32 J. Lv, M. Qin, X. Pang, L. Chen, Y. Liao, W. Wang, Y. Liu, S. Li, Z. Wang and W. Wu, Molecular mechanism of regulating tat protein expression of pingganjiedu TCM in the treatment of AIDS based on network pharmacology, *Int. J. Biol. Macromol.*, 2024, **278**, 134599.
33 A. G. B. Remorosa, P. W. Tsai, K. A. De Castro-Cruz, C. C. Hsueh, R. Y. Chen and B. Y. Chen, Deciphering characteristics of Macaranga tanarius leaves extract with electron shuttle-associated anti-inflammatory activity via microbial fuel cells, molecular docking, and network pharmacology, *Biochem. Eng. J.*, 2024, **208**, 109345.
34 L. H. Chin, C. M. Hon, D. K. Chellappan, J. Chellian, T. Madheswaran, F. Zeeshan, R. Awasthi, A. A. A. Aljabali, M. M. Tambuwala, H. Dureja, P. Negi, D. N. Kapoor, R. Goyal, K. R. Paudel, S. Satija, G. Gupta, A. Hsu, P. Wark, M. Mehta, R. Wadhwa, P. M. Hansbro and K. Dua, Molecular mechanisms of action of naringenin in chronic airway diseases, *Eur. J. Pharmacol.*, 2020, **879**, 173139.
35 X. Guo, R. R. Zhang, J. Y. Sun, Y. Liu, X. S. Yuan, Y. Y. Chen, H. Sun and C. Liu, The molecular mechanism of action for the potent antitumor component extracted using supercritical fluid extraction from Croton crassifolius root, *J. Ethnopharmacol.*, 2024, **327**, 117835.
36 C. Ren, L. Wang, X. Li, Y. Tang, X. Zhi, M. Zhuang, Q. Chen, X. Gao, X. Lv, C. Wang, X. Wu, K. Liu, X. Zhao and Y. Li, Elucidating the mechanism of action of radix angelica sinensis (Oliv.) diels and radix astragalus mongholicus bunge ultrafiltration extract on radiation-induced myocardial fibrosis based on network pharmacology and experimental research, *Eur. J. Pharm. Sci.*, 2024, **199**, 1066794.
37 Y. Zhu, F. Li, S. Wang, H. Shi, M. Zhao, S. You, S. Su and G. Cheng, Composite polysaccharide hydrogel loaded with scutellaria baicalensis extract for diabetic wound treatment, *Gels*, 2024, **23**, 605.
38 Y. Wang, T. Xu, X. Chen, Y. Ye, L. Liu, Y. Wang and P. Zhang, Network pharmacology and molecular docking approach to investigate the mechanism of a Chinese herbal formulation Yougui pills against steroid-related osteonecrosis of the femoral head, *Arabian J. Chem.*, 2024, **17**, 105609.
39 Z. Hu, J. Shan, X. Jin, W. Sun, L. Cheng, X. Chen and X. Wang, Nanoarchitectonics of in situ antibiotic-releasing acicular nanozymes for targeting and inducing cuproptosis-like death to eliminate drug-resistant bacteria, *ACS Nano*, 2024, **18**, 24327–24349.
40 W. Wang, Y. Cui, X. Wei, Y. Zang, X. Chen, L. Cheng and X. Wang, $CuCo_2O_4$ nanoflowers with multiple enzyme activities for treating bacterium-infected wounds via cuproptosis-like death, *ACS Nano*, 2024, **18**, 15845–15863.
41 W. Zhang, Y. Lv, Q. Niu, C. Zhu, H. Zhang, K. Fan and X. Wang, Zinc oxide-enhanced copper sulfide nanozymes promotethe healing of infected wounds by activating immune and inflammatory responses, *Small*, 2025, **21**, 2406356.
42 Y. Sun, W. Zhang, Z. Luo, C. Zhu, Y. Zhang, Z. Shu, C. Shen, X. Yao, Y. Wang and X. Wang, ZnO-CuS/F127 hydrogels with multienzyme properties for implant-related infection therapy by inhibiting bacterial arginine biosynthesis and promoting tissue repair, *Adv. Funct. Mater.*, 2025, **35**, 2415778.
43 L. Zhang, N. Chen, Y. Liao, Y. Kong, X. Yang, M. Zhan, W. Xu, Y. Wang, S. Zhu and Y. Hu, Efficacy and action mechanisms of compound Shen Chan decoction on experimental models of atopic dermatitis, *Int. Immunopharmacol.*, 2024, **137**, 112479.
44 K. S. Qu, Y. Ru, D. Yang, L. Kuai, Y. Luo, P. A. Zhang, M. Xing and H. F. Que, Fu-Huang ointment ameliorates impaired wound healing associated with diabetes through PI3K-AKT signalling pathway activation, *Comput. Biol. Med.*, 2023, **155**, 106660.